PanRep: Graph neural networks for extracting universal node embeddings in heterogeneous graphs.

Vassilis N. Ioannidis, Da Zheng, George Karypis

Abstract—**Learning unsupervised node embeddings facilitates several downstream tasks such as node classification and link prediction. A node embedding is universal if it is designed to be used by and benefit various downstream tasks. This work introduces PanRep, a graph neural network (GNN) model, for unsupervised learning of universal node representations for heterogenous graphs. PanRep consists of a GNN encoder that obtains node embeddings and four decoders, each capturing different topological and node feature properties. Abiding to these properties the novel unsupervised framework learns universal embeddings applicable to different downstream tasks. PanRep can be furthered fine-tuned to account for possible limited labels. In this operational setting PanRep is considered as a pretrained model for extracting node embeddings of heterogenous graph data. PanRep outperforms all unsupervised and certain semi-supervised methods in node classification and link prediction, especially when the labeled data for the semi-supervised methods is small. PanRep-FT (with fine-tuning) outperforms all other semi-supervised approaches, which corroborates the merits of pretraining models. Finally, we apply PanRep-FT for discovering novel drugs for Covid-19. We showcase the advantage of universal embeddings in drug repurposing and identify several drugs used in clinical trials as possible drug candidates.**

I. INTRODUCTION

Learning node representations from heterogeneous graph data powers the success of many downstream machine learning tasks such as node classification [1] and link prediction [2]. Graph neural networks (GNNs) learn node embeddings by applying a sequence of nonlinear operations parametrized by the graph adjacency matrix and achieve state-of-the-art performance in the aforementioned downstream tasks. The era of big data provides an opportunity for machine learning methods to harness large datasets [3]. Nevertheless, typically the labels in these datasets are scarce due to either lack of information or increased labeling costs [4]. The lack of labeled data points hinders the performance of supervised algorithms, which may not generalize well to unseen data and motivates *unsupervised* learning.

Unsupervised node embeddings may be used for downstream learning tasks, while the specific tasks are typically not known a priori. For example, node representations of the Amazon book graph can be employed for recommending new books as well as classifying a book's genre. Unsupervised learning can also be employed when limited labels of the downstream task are available in two ways. First, the node embeddings learned in the unsupervised setting can be used as fixed features in a supervised learning method that will train with

the limited labels. Such a two-stage approach will reduce the risk of overfitting since the node embeddings are not trained with the labels. Second, refining the unsupervised node embeddings with these labels could further increase the representation power of the embeddings. This can be achieved by *fine-tuning* the unsupervised model. In this setting, the GNN model is initialized with the trained model weights obtained by unsupervised learning. Next the model is extended by an output layer and trained for a few epochs with the available labels in an end-to-end fashion. Natural language processing methods have achieved state-of-the-art performance by applying such a fine-tuning framework [5]. Fine-tuning pretrained models is beneficial compared to end-to-end supervised learning since the former typically generalizes better especially when labeled data are limited and decreases the inference time since typically just a few fine-tuning iterations typically suffice for the model to converge [6]. In this work we will study both applications of unsupervised learning with limited label information.

This work aspires to provide *universal* node embeddings, which will be applied in multiple downstream tasks and achieve comparable performance to their supervised counterparts. The paper puts forth a novel framework for unsupervised learning of universal node representations on heterogenous graphs termed PanRep[1]. It consists of a GNN encoder that maps the heterogenous graph data to node embeddings and four decoders, each capturing different topological and node feature properties. The cluster and recover (CR) decoder exploits a clustering prior of the node attributes. The motif (Mot) decoder captures structural node properties that are encoded in the network motifs. The meta-path random walk (MRW) decoder promotes embedding similarity among nodes participating in a MRW and hence captures intermediate neighborhood structure. Finally, the heterogeneous information maximization (HIM) decoder aims at maximizing the mutual information among node local and the global representations per node type. These decoders model general properties of the graph data related to node homophily [7], [8] or node structural similarity [9], [10]. PanRep is solely supervised by the decoders and has no knowledge of the labels of the downstream task.

PanRep may utilize limited labels in two ways. First, the universal embeddings learned by PanRep are employed as features by models such as SVM [11] or DistMult [12] to be trained for the downstream tasks. Such an approach will reduce the risk of overfitting since the universal embeddings encode general properties of the graph data. Second, this paper also considers a fine-tuning PanRep (PanRep-FT) that inherits the

[1]Pan: Pangkosmios (Greek for universal) and Rep: Representation

weights of the PanRep model and employs an output layer for the label prediction. By selecting an appropriate output layer PanRep-FT accommodates arbitrary downstream tasks. In this operational setting, PanRep-FT is optimized adhering to a task-specific loss. PanRep can be considered as a pretrained model for extracting node embeddings of heterogenous graph data. Figure 1 illustrates the two novel models.

The contribution of this work is threefold.

C1. We introduce a novel problem formulation of universal unsupervised learning and design a tailored learning framework termed PanRep. We identify the following general properties of the heterogenous graph data: (i) the clustering of local node features, (ii) structural similarity among nodes, (iii) the local and intermediate neighborhood structure, (iv) and the mutual information among same-type nodes. We develop four tasks specific decoders to model the aforementioned properties.

C2. We extend the unsupervised universal learning framework to directly account for labels of the downstream task. By appropriately extending PanRep's architecture we can model arbitrary downstream learning tasks like node classification or link prediction. PanRep-FT refines the universal embeddings and increases the model generalization capability.

C3. We compare the proposed models to state-of-the-art semi-supervised and unsupervised methods for node classification and link prediction. PanRep outperforms all unsupervised and certain semi-supervised methods in node classification, especially when the labeled data for the semi-supervised methods is small. PanRep-FT outperforms even semi-supervised approaches in node classification and link prediction, which corroborates the merits of pretraining models. Finally, we apply our method on the drug-repurposing knowledge graph (DRKG) for discovering drugs for Covid-19 and identify several drugs used in clinical trials as possible drug candidates.

The rest of the paper is structured as follows. Sec. II introduces some related works to PanRep. Sec. III reviews some preliminaries to introduce the main paper. Sec. IV introduces the proposed PanRep model. The experimental setup is detailed in Sec. V. Finally, results and conclusions are presented in Secs. VI and VII, respectively.

II. RELATED WORK

Deep learning architectures typically process the input information using a succession of L hidden layers. Each of the layers comprises a conveniently parametrized linear transformation, a scalar nonlinear transformation, and possibly a dimensionality reduction (pooling) operator. By successively combining (non)linearly local features, the aim at a high level is to progressively extract useful information for learning [13], [14]. GNNs tailor these operations to the graph that supports the data [15], including the linear [16], and nonlinear [16], [17], [18], [19], [20], [21] operators. PanRep is an unsupervised GNN model that operates even in the absence of labeled data, whereas PanRep-FT provides a finetuned version of PanRep for supervised learning. The following sections introduce three research areas that this paper also explores with introducing relevant related work.

A. Unsupervised learning

Representation learning amounts to mapping nodes in an embedding space where the graph topological information and structure is preserved [22]. Typically, representation learning methods follow the encoder-decoder framework advocated by PanRep. Nevertheless, the decoder is typically attuned to a single task based on e.g., matrix factorization [23], [24], [25], [26], random walks [27], [28], or kernels on graphs [29]. Recently, methods relying on GNNs are increasingly popular for representation learning tasks [30]. GNNs typically rely on random walk-based objectives [27], [22] or on maximizing the mutual information among node representations [31]. Relational GNNs methods extend representation learning to heterogeneous graphs [32], [33], [34]. Relative to these contemporary works PanRep introduces multiple decoders to learn universal embeddings for heterogeneous graph data capturing the clustering of local node features, structural similarity among nodes, the local and intermediate neighborhood structure, and the mutual information among same-type nodes.

B. Supervised learning

Node classification is typically formulated as a semi-supervised learning (SSL) task over graphs, where the labels for a subset of nodes are available for training [35]. Graph-based SSL methods typically assume that the true labels are smooth over the graph, which naturally motivates leveraging the network topology to propagate the labels and increase learning performance. Graph-induced smoothness can be captured by graph kernels [36], [29], [37]; Gaussian random fields [38]; or low-rank parametric models [39], [40], [41], [42], [43]. GNNs achieve state-of-the-art performance in SSL by utilizing regular graph convolution [1] or graph attention [44], while these models have been extended in heterogeneous graphs [45], [46], [47].

Similarly, another prominent supervised downstream learning task is link prediction with numerous applications in recommendation systems [2] and drug discovery [48], [49]. Knowledge-graph (KG) embedding models rely on mapping the nodes and edges of the KG to a vector space by maximizing a score function for existing KG edges [2], [12], [50]. RGCN models [45] have been successful in link prediction and contrary to KG embedding models can further utilize node features. The universal embeddings extracted from PanRep without labeled supervision offer a strong competitive to these supervised approaches for both node classification and link prediction tasks.

C. Pretraining

Pretraining models provides a significant performance boost compared to traditional approaches in natural language processing [5] and computer vision [51], [52] . Pretraining offers increased generalization capability especially when the labeled data is scarce and increased inference speed relative to end-to-end training [5]. Parallel to our work [53], [54] proposed
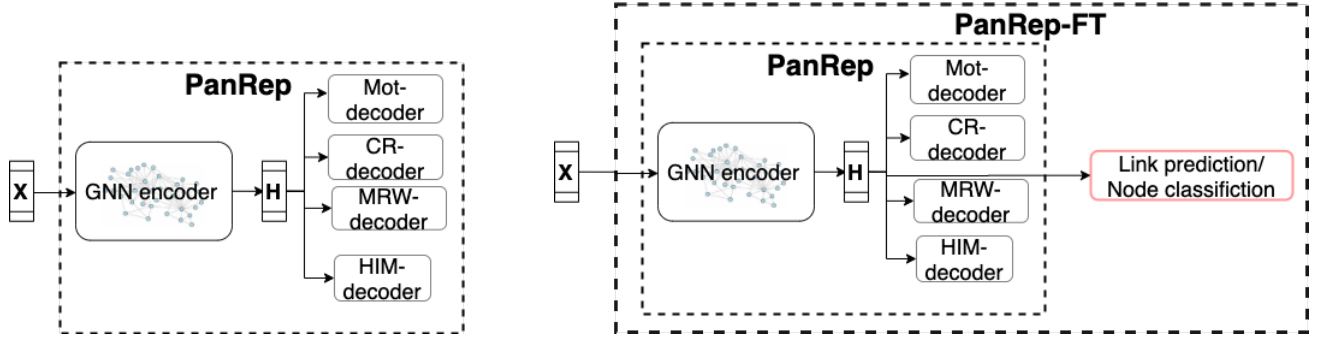
Fig. 1. Illustration of the PanRep (left) and PanRep-FT (right) models. The GNN encoder processes the node features $\mathbf{X}$ to obtain the embeddings $\mathbf{H}$. The decoders facilitate unsupervised learning of $\mathbf{H}$.

pretraining models for GNNs. These contemporary works supervise the models only using attribute or edge generation schemes without accounting for higher order structural similarity or maximizing the mutual information of the embeddings. Further, the work in [53] focuses solely on ranking objectives for evaluation. Recently, [55] introduced a framework for pretraining GNNs for graph classification. Different than [55] that focuses on graph representations, PanRep aims at node prediction tasks and obtains node representations via capturing properties related to node homophily [7] or node structural similarity [9]. PanRep is a novel pretrained model for node classification and link prediction that requires significantly less labeled points to reach the performance of its fully supervised counterparts.

III. DEFINITIONS AND NOTATION

Scalars are denoted by lowercase, column vectors by bold lowercase, and matrices by bold uppercase letters. Superscript $\cdot^{\top}$ denotes the transpose of a matrix; and $\text{diag}(\mathbf{x})$ corresponds to a diagonal matrix with the entries of $\mathbf{x}$ on its diagonal.

A heterogeneous graph with T node types and R relation types is defined as $\mathcal{G} := \{\{\mathcal{V}_t\}_{t=1}^T, \{\mathcal{E}_r\}_{r=1}^R\}^2$. The node types represent the different entities and the relation types represent how these entities are semantically associated to each other. For example, in the IMDB network, the node types correspond to actors, directors, movies, etc., whereas the relation types correspond to *directed-by* and *played-in* relations. The number of nodes of type t is denoted by N_t and its associated nodal set by $\mathcal{V}_t := \{n_t\}_{n=1}^{N_t}$. The total number of nodes in $\mathcal{G}$ is $N := \sum_{t=1}^t N_t$. The rth relation type, $\mathcal{E}_r := \{(n_t, r, n'_{t'}) \in \mathcal{V}_t \times \mathcal{V}_{t'}\}$, holds all interactions of a certain type among $\mathcal{V}_t$ and $\mathcal{V}_{t'}$ and may represent that a movie is *directed-by* a director. Heterogenous graphs are typically used to represent KGs [2].

Each node n_t is also associated with an $F \times 1$ feature vector $\mathbf{x}_{n_t}$. This feature may be a natural language embedding of the title of a movie. The nodal features are collected in a $N \times F$ matrix $\mathbf{X}$. Note that certain node types may not have features and for these we use an embedding layer to represent their features.

---

[2]This paper considers unweighted graphs that is the weight in the edge is either 0 or 1.

IV. PANREP

Given $\mathcal{G}$ and $\mathbf{X}$, our goal is to learn a function g such that $\mathbf{H} := g(\mathbf{X}, \mathcal{G})$, where $\mathbf{H} \in \mathbb{R}^{N \times D}$ represents the node embeddings and D is the size of the embedding space. Note that in estimating g, no labeled information is available.

Our work aims at universal representations $\mathbf{H}$ that perform well on different downstream tasks. Different node classification and link prediction tasks may arise by considering different number of training nodes and links and different label types, e.g., occupation label or education level label. Consider I downstream task, for the universal representations $\mathbf{H}$ it holds that

$$\mathcal{L}^{(i)}(f^{(i)}(\mathbf{H}), \mathcal{T}^{(i)}) \leq \epsilon, \; i = 1, \ldots, I, \tag{1}$$

where $\mathcal{L}^{(i)}$, $f^{(i)}$, and $\mathcal{T}^{(i)}$ represent the loss function, learned classifier, and training set (node labels or links) for task i, respectively and ϵ is the largest error for all tasks. The goal of unsupervised universal representation learning is to learn $\mathbf{H}$ such that ϵ is small. While learning $\mathbf{H}$, PanRep does not have knowledge of $\{\mathcal{L}^{(i)}, f^{(i)}, \mathcal{T}^{(i)}\}_i$. Nevertheless, by utilizing the novel decoder scheme PanRep achieves superior performance even compared to supervised approaches across tasks.

Our universal representation learning framework aims at embedding nodes in a low-dimensional space such that the representations are discriminative for node classification and link prediction. PanRep utilizes an GNN encoder that maps the node features and graph structure to node embeddings $\mathbf{H}$ that is detailed in Sec. IV-A. The node embedding matrix $\mathbf{H}$ is the input to four decoders each capturing unique graph properties; see Sec. IV-B. The combined loss of the decoders trains PanRep in an end-to-end fashion. A task specific loss function for node classification and link prediction extends PanRep to supervised learning settings and gives rise to PanRep-FT in Sec. IV-C. Figure 1 provides an illustration of the overall PanRep architecture. Different than existing approaches, PanRep combines multiple decoders in a multi-task learning scheme to learn node embedding that perform well in a variety of tasks.

A. PanRep Encoder

The abundance of graph-abiding data calls for advanced learning techniques that complement nicely standard machine

learning tools when the latter cannot be directly employed, e.g. due to irregular data inter-dependencies. Permeating the benefits of deep learning to graph data, graph neural networks (GNNs) offer a versatile and powerful framework to learn from complex graph data [15].

The GNN layer operates per node n in the graph and performs 3 steps: 1) aggregates the input embeddings corresponding to the neighbors of n, 2) Projects the combined embedding to a new vector via a parametrized projection matrix $\mathbf{W}$, and 3) Nonlinearly transforms the projected embedding. Different GNN models employ variations of these steps. Although the PanRep framework can utilize any GNN model as an encoder [30], in this paper PanRep uses a relational graph convolutional network (RGCN) encoder [45]. RGCNs extend the graph convolution operation [1] to heterogenous graphs. The lth RGCN layer computes the nth node representation $\mathbf{h}_n^{(l+1)}$ as follows

$$\mathbf{h}_n^{(l+1)} := \sigma \left(\sum_{r=1}^{R} \sum_{n' \in \mathcal{N}_n^r} \mathbf{h}_{n'}^{(l)} \mathbf{W}_r^{(l)} \right), \qquad (2)$$

where $\mathcal{N}_n^r$ is the neighborhood of node n under relation r, σ the rectified linear unit non linear function, and $\mathbf{W}_r^{(l)}$ is a learnable matrix associated with the rth relation. Essentially, the output of the RGCN layer for node n is a nonlinear combination of the hidden representations of neighboring nodes weighted based on the relation type. The node features are the input of the first layer in the model i.e., $\mathbf{h}_n^{(0)} = \mathbf{x}_n$, where $\mathbf{x}_n$ is the node feature for node n. The matrix $\mathbf{H}$ in this paper represents the embedding extracted in the final layer.

Recent studies [56], [57] manage to unify different GNN variants into the message passing paradigm. The RGCN layer in 2 can be interpreted under this framework where each node n collects the messages send by his neighbors $\mathbf{h}_{n'}^{(l)}$ and transforms them. By implementing the message passing paradigm the deep graph learning (DGL)[3] library provides highly optimized GNN models [58].

B. Universal supervision decoders

Methods for learning over graphs typically rely on modeling homophily of nodes that postulates neighboring vertices to have similar attributes [29], [59] or structural similarity among nodes [9], where vertices involved in similar graph structural patterns possess related attributes [10].

Motivated by these methods we identify related properties encoded in the graph data. Clustering nodes based on their attributes provides a strong signal for node homophily [60]. Network motifs reveal the local structure information for nodes in the graph [61]. Metapaths encode the heterogeneous graph neighborhood and indicate the local connectivity [32]. Finally, maximizing the mutual information among embeddings declusters node representations and provides further discriminative information [31]. Towards capturing the aforementioned properties, we develop four novel neural network based decoders. PanRep's encoder computes the embedding matrix
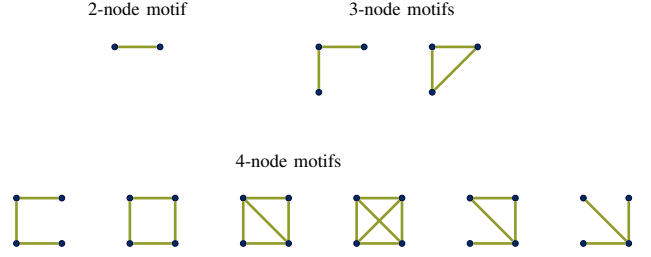
[3]https://www.dgl.ai/

Fig. 2. Connected motifs up to size 4 nodes. The motif frequency $\boldsymbol{\mu}_n$ shows how many times node n exits in the corresponding motifs.

$\mathbf{H}$ that is fed to the decoders, which supervise the learning by promoting graph properties in $\mathbf{H}$.

1) Cluster and recover supervision: Node attributes may reveal interesting properties of nodes, such as clusters of customers based on their buying power and age. This is important in recommendation systems, where traditional matrix factorization approaches [60] rely on revealing clusters of similar buyers. To capitalize such information we propose to supervise the universal embeddings by such cluster representations. Specifically, we cluster the node attributes via K-means [62] and then design a model that decodes $\mathbf{H}$ to recover the original clusters. The CR-decoder amounts to a single layer multilayer perceptron (MLP) as follows

$$\hat{\mathbf{C}} := \sigma(\mathbf{H}\mathbf{W}_{\text{CR}}), \qquad (3)$$

where $\hat{\mathbf{C}}$ is a $N \times K$ matrix representing the output of the decoder and $\mathbf{W}_{\text{CR}}$ is a learnable matrix. The task specific loss function for this decoder is

$$\mathcal{L}_{\text{CR}} := - \sum_{n=1}^{N} \sum_{k=1}^{K} C_{nk} \ln \hat{C}_{nk}, \qquad (4)$$

where the cluster assignment C_{nk} is 1 if node n belongs in class k and the predicted cluster assignment $\hat{C}_{nk}$ is the output of the CR-decoder. We showcase in the experiments that this decoder is superior to the attribute generation scheme used in [53]. Such a supervision decoder will enrich the universal embeddings $\mathbf{H}$ with information based on the clustering of local node features.

2) Motif supervision: Network motifs are sub-graphs where the nodes have specific connectivity patterns. Typical size-3 motifs for example, are the triangle and the star motifs. Each of these sub-graphs conforms to a particular pattern of interactions among nodes, and reveals important properties for the participating nodes. In gene regulatory networks for example, motifs relate to certain biological properties [63]. The work in [61] develops efficient parallel implementations for extracting network motifs. We aspire to capture structural similarity among nodes by predicting their motif information. The motivation is that nodes which might be distant in the graph may have similar structural properties as described by their motifs.

Using the method in [61] we extract a $M \times 1$ frequency vector $\boldsymbol{\mu}_n$ per node that shows how many times the node n participates in motifs of size up to 4 nodes. Fig. 2 shows the different motifs up to size 4. This information reveals the

structural role of nodes such as star-center, star-edge nodes, or bridge nodes. The motif decoder predicts this vector for all nodes using the universal representation $\mathbf{H}$. This allows for information sharing among nodes which are far away in the graph but have similar motif frequency vectors. The motif decoder utilizes a single layer MLP as follows

$$\hat{\boldsymbol{\mu}}_n := \sigma(\mathbf{h}_n \mathbf{W}_{\mathrm{MOT}}), \quad n = 1, \dots, N, \tag{5}$$

where $\hat{\boldsymbol{\mu}}_n$ is a $M \times 1$ matrix representing the output of the decoder and $\mathbf{W}_{\mathrm{MOT}}$ is a $D \times M$ learnable matrix. The motif decoder optimizes the following loss function

$$\mathcal{L}_{\mathrm{MOT}} := \sum_{n=1}^{N} \|\boldsymbol{\mu}_n - \hat{\boldsymbol{\mu}}_n\|_2^2, \tag{6}$$

where $\hat{\boldsymbol{\mu}}_n$ is the output of the Mot-decoder for the nth node. Using the Mot-decoder PanRep enhances the universal embeddings by structural information encoded in the node motifs.

3) Metapath RW supervision: Metapaths are sequences of edges of possibly different type that connect nodes in a KG. A metapath random walk (MRW) is a specialized RW that follows different edge-types [32].

We aspire to capture local connectivity patterns by promoting nodes participating in a MRW to have similar embeddings. Consider all node pairs for nodes $(n_t, n'_{t'})$ participating in a MRW, the following criterion maximizes the similarity among these nodes as follows

$$\mathcal{L}_{\mathrm{MRW}} := \log(1 + \exp(-y \times \mathbf{h}_{n_t}^{\top} \mathrm{diag}(\mathbf{r}_{t,t'}) \mathbf{h}_{n'_{t'}})), \tag{7}$$

where $\mathbf{h}_{n_t}$ and $\mathbf{h}_{n'_{t'}}$ are the universal embeddings for nodes n_t and $n'_{t'}$, respectively, $\mathbf{r}_{t,t'}$ is an embedding parametrized on the pair of node-types and y is 1 if n_t and $n'_{t'}$ co-occur in the MRW and -1 otherwise. Negative examples are generated by randomly selecting tail nodes for a fixed head node with ratio 5 negatives per positive example.

Metapaths convey more information than regular links since the former can be defined to promote certain prior knowledge. For example, in predicting the movie genre in IMDB the metapath configured by the edge types (played by, played in) among node types (movie, actor, movie) will potentially connect movies with same genre, which will allow the PanRep to map such movies to similar embeddings and hence it is desirable. The embedding per node-type pair $\mathbf{r}_{t,t'}$ allows the MRW-decoder to weight the similarity among node embeddings from different node types accordingly. The length of the MRW controls the radius of the graph neighborhood in equation (7) and it can vary from local to intermediate. Note that link prediction is a special case of MRW supervision that considers MRWs of length 1.

4) Heterogenous information maximization: The aforementioned supervision decoders capture clustering affinity, structural similarity and local and intermediate neighborhood of the nodes. Nevertheless, further information can be extracted by the representations by maximizing the mutual information among node representations. Such an approach for homogeneous graphs is detailed in [31], where the mutual information

between node representations and the global graph summaries is maximized [64].

Towards further refining the universal embeddings, we propose a generalization of [31] for heterogeneous graphs. We consider a global summary vector per t as $\mathbf{s}_t := \sum_{n_t=1}^{N_t} \mathbf{h}_{n_t}$ that captures the average tth node representation. We aspire to maximize the mutual information among $\mathbf{s}_t$ and the corresponding nodes in $\mathcal{V}_t$. The proposed HIM decoder optimizes the following contrastive loss function

$$\mathcal{L}_{\mathrm{HIM}} := \sum_{t=1}^{T} \Bigg(\sum_{n_t=1}^{N_t} \log \left(\sigma(\mathbf{h}_{n_t}^{\top} \mathbf{W} \mathbf{s}_t) \right) \\ + \log \left(1 - \sigma(\tilde{\mathbf{h}}_{n_t}^{\top} \mathbf{W} \mathbf{s}_t) \right) \Bigg), \tag{8}$$

where the bilinear scoring function $\sigma(\tilde{\mathbf{h}}_{n_t}^{\top} \mathbf{W} \mathbf{s}_t)$ captures how close is $\mathbf{h}_{n_t}$ to the global summary, $\mathbf{W}$ is a learnable matrix and $\tilde{\mathbf{h}}_{n_t}$ represents the negative example used to facilitate training. Designing negative examples is a cornerstone property for training contrastive models [31]. We generate the negative examples in (8) by shuffling node attributes among nodes of the same type. The HIM decoder maximizes the mutual information across nodes and complements the former decoders.

5) The overall loss function: RGCN extracts the embedding matrix $\mathbf{H}$ that is the input to the decoders presented in IV-B. PanRep's overall loss function is the linear combination of (4), (6), (7), and (8)

$$\mathcal{L} := \mathcal{L}_{\mathrm{CR}} + \mathcal{L}_{\mathrm{MOT}} + \mathcal{L}_{\mathrm{MRW}} + \mathcal{L}_{\mathrm{HIM}}. \tag{9}$$

A backpropagation algorithm [65] minimizes (9). The objective also relates to the framework of deep multitask learning [66], since the GNN encoder is shared across the multiple supervision tasks and PanRep makes multiple inferences in one forward pass. Such networks are not only scalable, but the shared features within these networks can induce more robust regularization and possibly boost performance [67]. Introducing adaptive weights per decoder to control its learning rate is a future direction of PanRep.

C. PanRep-FT

In certain cases a subset of labels may be known a priori for the downstream task and it is beneficial to fine-tune PanRep's model to obtain refined node representations. In this context, PanRep is a pretrained model and a downstream task specific loss can further supervise PanRep. First, we train PanRep for some epochs using the unsupervised decoders in Sec. IV-B and then we train PanRep's encoder for some epochs solely on the downstream task specific loss. Fig. 1 illustrates on the right side the PanRep-FT framework. Next, we present the supervised tasks along with their corresponding problem formulations and training losses.

1) Node classification: Node classification has numerous applications and gives rise a SSL task over graphs, where given the features $\mathbf{X}$, the graph structure $\mathcal{G}$, and the labels for a subset of nodes the goal is to predict the labels across all nodes [35].

Each node n has a label $y_n \in \{0, \dots, P-1\}$, which in the IMDB network may represent the genre of a movie. In SSL, we

know labels only for a subset of nodes $\{y_n\}_{n \in \mathcal{M}}$, with $\mathcal{M} \subset \mathcal{V}$. This partial availability may be attributed to privacy concerns (medical data); energy considerations (sensor networks); or unrated items (recommender systems). The $N \times P$ matrix $\mathbf{Y}$ is the one-hot representation of the true nodal labels; that is, if $y_n = p$ then $Y_{n,p} = 1$ and $Y_{n,p'} = 0, \forall p' \neq p$.

Given the universal embeddings $\mathbf{H}$ PanRep-FT employs a single layer MLP to obtain the predicted label matrix $\hat{\mathbf{Y}}$ as follows

$$\hat{\mathbf{Y}} := \mathbf{H}\mathbf{W}_{\text{NC}}, \tag{10}$$

where the projection matrix $\mathbf{W}_{\text{NC}}$ is a learnable parameter, $\hat{\mathbf{Y}}$ is an $N \times K$ matrix, and $\hat{Y}_{n,k}$ represents the probability that $y_n = k$. PanRep-FT loss function for this node classification (nc) task is a cross-entropy loss

$$\mathcal{L}_{\text{NC}} := - \sum_{n \in \mathcal{M}} \sum_{p=1}^{P} Y_{np} \ln \hat{Y}_{np}, \tag{11}$$

where the error is averaged over the nodes with labels in $\mathcal{M}$. The loss function in (11) will force PanRep's encoder to learn suitable parameters to minimize the classification error. After training the matrix $\hat{\mathbf{Y}}$ from the output function in (10) predicts the class of the unlabeled nodes.

2) Link prediction: Consider the heterogeneous graph $\mathcal{G}$ in Sec. III. Given the sets of links $\{\mathcal{E}_r\}_{r=1}^{R}$, and the node features $\mathbf{X}$ the goal of link prediction is to predict whether a set of links different than the one used for training might exist or not in the graph.

Typically, link prediction models utilize a contrastive loss function that requires the model to distinguish among positive and negative examples [50]. In this context, positive examples are the set of existing links in the graph. The negative examples, which are links that the model should classify as nonexistent, are typically sampled from the missing links in the graph. For each *positive triplet* $q = (n_t, r, n'_{t'})$ a number of negative links is generated by corrupting the head and tail entities at random $(n_t, r, \nu'_{t'})$ and $(\nu_t, r, n'_{t'})$. This paper considers 5 negative examples per one positive for link prediction.

PanRep-FT employs a DistMult model [12] for link prediction. The loss function is

$$\min \sum_{(n_t, r, n'_{t'}) \in \mathbb{D}^+ \cup \mathbb{D}^-} \log(1 + \exp(-y \times \mathbf{h}_{n_t}^\top \text{diag}(\mathbf{h}_r) \mathbf{h}_{n'_{t'}})), \tag{12}$$

where $\mathbf{h}_{n_t}$ and $\mathbf{h}_{n'_{t'}}$ are the embedding of the head and tail entity n_t, $n'_{t'}$ obtained by PanRep's encoder and $\mathbf{h}_r$ is a trainable parameter corresponding to relation r that is directly from (12). The scalar represented by $\mathbf{h}_{n_t}^\top \text{diag}(\mathbf{h}_r) \mathbf{h}_{n'_{t'}}$ denotes the score of triplet $(n_t, r, n'_{t'})$ as given by the DistMult model [12]. Finally, $\mathbb{D}^+$ and $\mathbb{D}^-$ are the positive and negative sets of triplets and $y = 1$ if the triplet corresponds to a positive example and -1 otherwise. By minimizing (12) PanRep-FT will learn node embeddings $\mathbf{H}$, which will be informative for link prediction. PanRep-FT predicts new links by calculating their DistMult score; see also Sec. V-C.

Pretraining PanRep before applying the task specific loss functions may increase the model performance. BERT models

in natural language processing have reported state of the art results by considering such a pretrain and fine-tune framework [5]. PanRep-FT is a counterpart of BERT for extracting information from heterogenous graph data. PanRep-FT combines the benefit of universal unsupervised learning and task specific information and achieves greater generalization capacity especially when labeled data are scarce [6].

Alternative encoders. Several works consider designing possibly more general GNN encoders that utilize attention mechanism [47], [44] or graph isomorphism networks [68]. This paper proposes novel supervision decoders for unsupervised learning that capture general properties of the graph data. Designing a universal encoder based on these contemporary GNN models is a future direction of PanRep.

V. Experimental setup

We implement PanRep in the efficient deep graph learning (DGL)[4] library [58]. PanRep experiments run on an AWS P3.8xlarge instances with 8 GPUs each having 16GB of memory[5].

A. Methods

Our universal representation learning techniques compares against with state-of-the-art methods. For node classification consider the following contemporary methods RGCN [45], HAN [47], MAGNN [46], node2vec [27], meta2vec [32] and an adaptations of the work in [31] for heterogenous graphs termed HIM. The competing methods RGCN, MAGNN and HAN also use the DGL. For link prediction the baseline models is RGCN [45] with DistMult supervision [12] that uses the same encoder as PanRep.

The parameters for all methods considered optimize the performance on the validation set. For PanRep the Mot-decoder and RC-decoder employ a 1-layer MLP. For the MRW-decoder we use length-2 MRWs. For the majority of the experiments PanRep uses a hidden dimension of 300, 1 hidden layer, 800 epochs of model training, 100 epochs for finetuning, and an ADAM optimzer [69] with a learning rate of 0.001. For link prediction finetuning PanRep uses a DistMult model [12] whereas for node classification it uses a logistic loss.

B. Datasets

We consider a subset of the IMDB dataset [70] containing 11,616 nodes belonging to three node-types and 17,106 edges belonging to six edge-types. Each movie is associated with a label representing its genre and with a feature vector corresponding to its keywords. We also use a subset of the OAG dataset [71] with 23,696 nodes belonging to four node-types (authors, affiliations, papers, venues) and 90,183 edges belonging to 14 edge-types. In OAG we did not use MOT supervision since the graph does not have a rich motif structure. Each paper is associated with a label denoting the scientific area and with an embedding of the papers' text. Table I provides additional information about these two datasets.

[4]https://www.dgl.ai/
[5]https://aws.amazon.com/ec2/instance-types/p3/

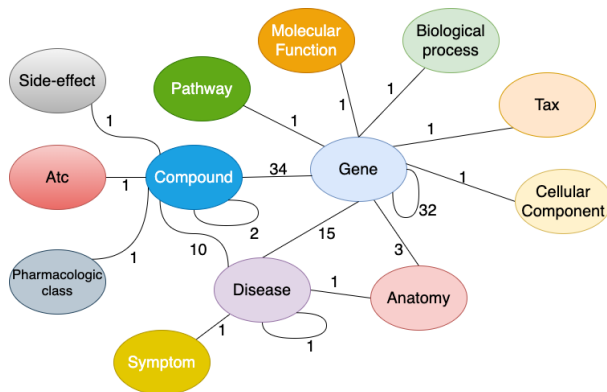| Dataset	Node type	Nodes	Edge type	Edges
IMDB	Movie (M)	4,278	M-directed by-D	4,278
	Director (D)	2,081	M-played by-A	12,828
	Actor (A)	5,25		
OAG	Author (A)	13,720	A-writes as last-P	4,522
	Paper (P)	7,326	P-in journal-V	3,941
	Affiliation (Af)	2,290	P-conference-V	3,368
	Venue (V)	782	P-cites-P	3,327
			A-writes as other-P	7,769
			A-writes as first-P	4,795
			A-affiliated with-Af	17,035

Fig. 3. The schema of the Drug Repurposing Knowledge Graph (DRKG). The number next to an edge indicates the number of relation-types among the corresponding entity types in the DRKG.

In addition, we use a third dataset corresponding to the drug repurposing knowledge graph (DRKG) constructed in [49]. DRKG, whose schema is shown in Figure 3, contains 5,874,261 biological interactions belonging to 107 edge-types and 97,238 biological entities from 13 entity-types. DRKG is used for evaluating link-prediction tasks.

C. Evaluation metrics

For evaluating node classification methods we use macro and micro F1 score that is advantageous when the classes are unbalanced [72]. The F1 score is the harmonic mean of the precision and recall and reaches its best value at 1 and worst value at 0. The Mirco-F1 score calculates the metric across labels by counting the total true positives, false negatives and false positives. The Macro-F1 calculate metrics for each label, and find their unweighted mean. This does not take label imbalance into account.

Link prediction evaluation utilizes two standard criteria the Hit-10 and Mean Reciprocal Rank (MRR) metrics [73], [74], [50]. Both metrics are derived by comparing how the score of the positive triplet relates to the scores of its associated negative instances.

For each *positive triplet* $q = (n_t, r, n'_{t'})$ we generate all possible triplets of the form $(n_t, r, \nu'_{t'})$ and $(\nu_t, r, n'_{t'})$ by corrupting the head and tail entities. We then removed from them any triplets that already exist in the dataset. The set of

triplets that remained form the *negative triplets* associated with the initial positive triplet. The positive and negative triplets are then scored by the DistMult [12] model in (12).

We construct a list of triples S_q containing q and its associated negative triplets that order them in a non-increasing score fashion, and let $rank_q$ be qth's position in S_q. Given that, Hit-10 is the average number of times the positive triplet is among the 10 highest ranked triplets, whereas MRR is the average reciprocal rank of the positive instances. Mathematically, the metrics are as follows

$$\text{Hit-10} := \frac{1}{Q}\sum_{q=1}^{Q} \mathbb{1}_{rank_q \leq 10}, \quad \text{MRR} := \frac{1}{Q}\sum_{q=1}^{Q}\frac{1}{rank_q},$$

where Q is the total number of positive triplets and $\mathbb{1}_{rank_q \leq 10}$ is 1 if $rank_q \leq 10$, otherwise it is 0. Note that Hit-10 and MRR are between 0 and 1, with values closer to 1 corresponding to better predictions.

D. Scalability

PanRep is implemented using DGL's mini-batch training, which is scalable w.r.t. time and space. During mini-batch training a subset of seed nodes is sampled along with the K-hop neighbors of the seed nodes, where K is the depth of the GNN. Furthermore, the number of edges at each level is bounded by using neighbor sampling. This allows training on graphs with billions of nodes/edges since only a fraction of the nodes/edges will be loaded on the GPU per mini-batch. PanRep's complexity is controlled by the RGCN encoder whose computation complexity of a mini-batch is $\mathcal{O}(BF^K)$ for sparse graphs, where B is the batch size, K is the number of layers and F is the maximum number of neighbors per node. By using neighbor sampling, F is usually less than 10–20 and in our experiments we found that K=2 often works well. The decoders' complexity is significantly lower and do not add but a constant factor to the overal complexity and hence the overall per-epoch runtime is similar to that of RGCN.

VI. RESULTS

A. Node classification

In this experiment we compare semi-supervised and unsupervised methods for classification. First, the labeled nodes are split in 10% training, 5% validation, and 85% testing sets. The semi-supervised methods utilize the training labels whereas the unsupervised methods do not use them in calculating the node embeddings. Then the embeddings corresponding to the 85% testing nodes are further split to training and testing sets and a linear support vector machine (SVM) is trained on the training set for evaluation following the setup in [46]. The reason that we selected a simple linear classifier as the SVM over a potentially more powerful non-linear one, e.g., an multi-layer perception (MLP) classifier, is because an SVM classifier allows us to directly compare the representation power of the different approaches, whereas an MLP classifier that employs a neural network will enhance the representation power of certain methods and result to unfair comparisons.

TABLE II
NODE CLASSIFICATION RESULTS.

	Train %		Unsupervised				Semi-supervised			
			node2vec	meta2vec	HIM	PanRep	HAN	MAGNN	RGCN	PanRep-FT
IMDB	Macro-F1	40%	50.63	47.57	55.21	**56.04**	56.15	**60.27**	58.48	59.49
		60%	51.65	48.17	57.66	**58.51**	57.29	**60.66**	58.42	59.86
		80%	51.49	49.99	57.89	**60.23**	58.51	61.44	58.76	**61.49**
	Micro-F1	40%	51.77	48.17	55.11	**55.92**	57.32	**60.50**	58.64	59.67
		60%	52.79	49.87	56.57	**58.41**	58.42	**60.88**	58.55	59.75
		80%	52.72	50.50	57.79	**60.14**	59.24	61.53	58.89	**61.59**
OAG	Macro-F1	40%	56.37	**65.75**	50.54	57.76	63.99	63.31	64.68	**64.72**
		60%	57.01	**66.09**	51.98	59.72	64.25	63.42	65.96	**66.99**
		80%	58.05	**65.75**	53.25	63.03	64.37	63.89	67.67	**67.90**
	Micro-F1	40%	70.17	74.54	71.91	**75.50**	73.95	72.74	**81.92**	80.36
		60%	70.95	74.96	73.89	**77.39**	75.32	72.75	81.39	**81.78**
		80%	72.24	74.73	75.31	**79.76**	75.24	73.43	82.38	**83.17**

TABLE III
NODE CLASSIFICATION RESULTS FOR DIFFERENT LABELED SUPERVISION SPLITS.

Datasets	Metrics	Train embeddings %		5%		10%		20%	
		Train%	PanRep	RGCN	PanRep-FT	RGCN	PanRep-FT	RGCN	PanRep-FT
IMDB	Macro-F1	40%	56.04	55.12	**56.85**	58.48	**59.49**	61.30	**63.14**
		60%	58.51	55.20	**59.39**	58.42	**59.86**	60.98	**62.91**
		80%	60.23	55.55	**61.27**	58.76	**61.49**	61.10	**62.72**
	Micro-F1	40%	55.92	55.27	**56.92**	58.64	**59.67**	61.49	**63.17**
		60%	58.41	55.39	**59.45**	58.55	**59.75**	61.17	**62.89**
		80%	60.14	55.62	**61.32**	58.89	**61.39**	61.30	**62.75**
OAG	Macro-F1	40%	57.76	55.51	**64.99**	64.68	**64.72**	67.07	65.31
		60%	59.72	55.99	**66.62**	65.96	**66.99**	67.58	66.25
		80%	63.03	56.36	**68.94**	66.10	**68.60**	67.67	**67.90**
	Micro-F1	40%	75.50	78.00	**80.19**	81.92	80.36	82.57	81.17
		60%	77.39	78.07	**81.36**	81.39	**81.78**	81.74	81.34
		80%	79.76	78.44	**82.52**	82.38	**83.17**	82.20	**82.31**

We report the Macro and Micro F1 accuracy for different training percentages of the 85% nodes fed to the SVM classifier in Table II. First, PanRep outperforms other unsupervised approaches as well as some semi-supervised approaches. In the 80% splits, PanRep outperforms even its semi-supervised counterpart RGCN that uses node labels for supervision. Metapath2vec [32] reports competitive performance for OAG in Macro-F1 score but underperforms in Micro-F1. Nevertheless, in this experiment Metapath2vec only uses the best performing metapath that is *paper-venue-paper*, which is considerably better than that of most other metapaths. This way of selecting the metapath, gives Meta2vec an (unfair) advantage over PanRep, which uses all metapaths of length 2 as it computes a universal representation (along with the other supervision decoders). PanRep-FT outperforms RGCN that uses the same encoder, which is a testament to the power of pretraining models. Finally, PanRep-FT matches and outperforms in certain splits the state-of-the-art MAGNN that uses a more expressive encoder. PanRep's universal decoders enhance the embeddings with additional discriminative power that results to improved performance in the downstream tasks.

Table III reports the accuracy of the PanRep-FT and the encoder RGCN, which is trained directly for the semi-supervised learning task to obtain the embeddings. PanRep-FT consistently outperforms RGCN across most SVM splits, whereas PanRep-FT's advantage over RGCN decreases as more training data for the embeddings are available; see e.g., the last column with 20% training, which is justifiable since more

labels diminish the advantage of pretraining.[6] Moreover even without labeled supervision the unsupervised embeddings of PanRep outperform the semi-supervised RGCN embeddings for 5% training labels. This demonstrates the importance of using PanRep as a pretraining method. Finally, RGCN reports similar performance across SVM training splits for all columns, whereas PanRep-FT increases with more supervision. These results suggest that PanRep-FT's embeddings have higher generalization capacity.

B. Link prediction

Our universal embedding framework is further evaluated for link prediction using the IMDB and OAG datasets. The MRW decoder is used to evaluate the performance of PanRep in link prediction. Specifically, the MRW score calculated by the scaled inner product $\mathbf{h}_{n_t}^\top \mathrm{diag}(\mathbf{r}_{t,t'})\mathbf{h}_{n'_{t'}}$ in (7) is used to predict whether there exists a link between the nodes n_t and n'_{t}; see also Sec.V-C for details on the link prediction evaluation. In this section, we utilize a percentage $x\%$ of all the links in the graph to train the methods and the rest $95 - x\%$ to test the approaches, while holding 5% for validation.

Figures 4 and 5 report the MRR and Hit-10 scores of the baseline methods along with the PanRep and PanRep-FT methods. We report the performance of the methods for different percentages of links used for training. Observe that PanRep-FT consistently outperforms the competing methods

---

[6] PanRep-FT performs only 100 finetuning epochs with labeled supervision, which is significantly less to the 800 epochs of labeled supervision by RGCN.

TABLE IV
ABLATION STUDY FOR DIFFERENT SUPERVISION DECODERS.

| Datasets	Metrics	Train %	HIM	MRW	HIM+MRW	MOT	CR	PanRep
IMDB	Macro-F1	40%	55.21	54.54	55.32	42.28	32.21	**56.04**
		60%	57.66	56.12	57.24	43.41	35.16	**58.51**
		80%	57.89	56.64	57.74	44.31	35.66	**60.23**
	Micro-F1	40%	55.11	54.36	55.53	43.66	39.13	**55.92**
		60%	56.57	55.91	56.25	44.89	40.03	**58.41**
		80%	57.79	56.49	58.42	45.65	40.66	**60.14**
OAG	Macro-F1	40%	50.54	55.92	56.11	-	15.46	**57.76**
		60%	51.98	58.40	58.91	-	15.48	**59.72**
		80%	53.25	60.61	61.74	-	15.54	**63.03**
	Micro-F1	40%	71.91	74.39	74.65	-	63.06	**75.50**
		60%	73.89	76.76	76.33	-	63.14	**77.39**
		80%	75.31	78.90	78.71	-	63.59	**79.76**
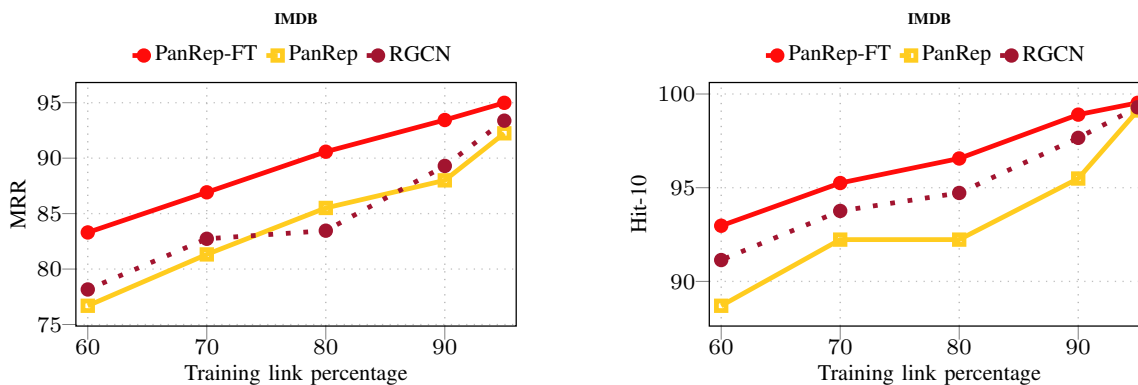
Fig. 4. MRR and Hit-10 for link prediction across different percentages of testing links for IMDB.
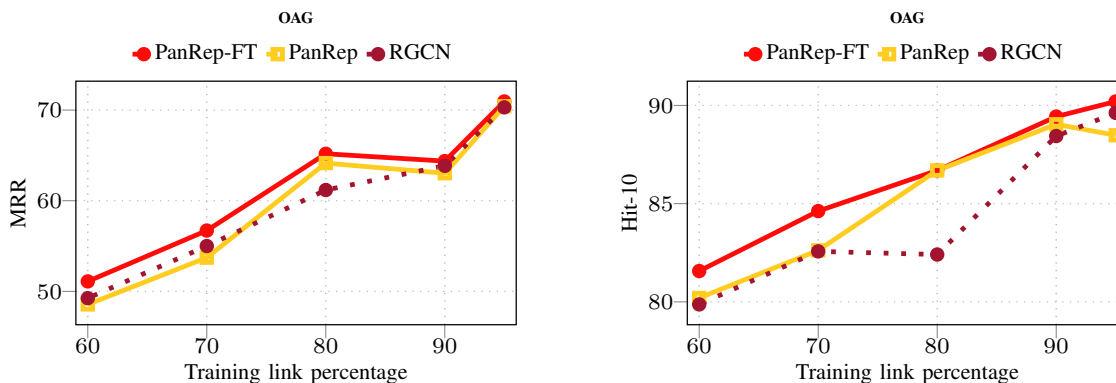

Fig. 5. MRR and Hit-10 for link prediction across different percentages of testing links for OAG.

and the performance gain increases as the percentage of training links decreases. This corroborates the advantage of pretraining GNNs for link prediction. Note that PanRep that is trained on MRW decoder which resembles the link prediction task reports similar performance with RGCN that is trained solely in link prediction. For few training data PanRep outperforms RGCN whereas as the training data increases RGCN reduces the gap in performance and eventually outperforms PanRep. This competitive performance of PanRep highlights the use of the other decoders that regularize learning and corroborate to the success of the universal embeddings in link prediction.

1) Drug repurposing: Drug-repurposing aims at discovering the most effective existing drugs to treat a certain disease.

We formulate drug-repurposing as a link prediction task, where we are trying to recover the appropriate drug nodes to link to a disease node. The Drug Repurposing Knowledge Graph (DRKG) [49] collects interactions from a collection of biological databases such as Drugbank [75], STRING [76], IntAct [77] and DGIdb [78].

We put forth drug-repurposing as predicting direct links in the DRKG. Here, we attempt to predict whether a drug inhibits a certain gene, which is related to the target disease. We identify 442 genes that relate to the Covid-19 disease. We select 8,104 FDA-approved drugs in the DRKG as candidates. Our work focused entirely on *evaluating* the ranked list of candidate drugs against a set of 32 drugs that, at the time of submission, were

TABLE V
DRUG INHIBITS GENE SCORES FOR COVID-19.

PanRep-FT		RGCN	
Drug name	# hits	Drug name	# hits
Losartan	232	Chloroquine	69
Chloroquine	198	Colchicine	41
Deferoxamine	104	Tetrandrine	40
Ribavirin	101	Oseltamivir	37
Methylprednisolone	44	Azithromycin	36
Thalidomide	41	Tofacitinib	33
Hydroxychloroquine	19	Ribavirin	32
Tetrandrine	13	Methylprednisolone	30
Eculizumab	10	Deferoxamine	30
Tocilizumab	9	Thalidomide	25
Dexamethasone	7	Dexamethasone	24
Azithromycin	6	Bevacizumab	21
Nivolumab	5	Hydroxychloroquine	19
Piclidenoson	5	Losartan	19
Oseltamivir	5	Ruxolitinib	13
		Eculizumab	12
		Sarilumab	8
		Baricitinib	6

in Covid-19 clinical trials [79], [48]. Specifically, given a gene whose associated protein is a potential drug target, we rank the 8104 FDA approved drugs and select the 100 highest ranked drugs. We evaluated the performance of a method by looking at the intersection between these 100 highest ranked drugs and the 32 drugs in Covid-19 trials. In our experiments, we used 442 genes that researchers have identified as potential targets for Covid-19 and computed 442 ranked lists and associated intersections. We aggregated the results by counting the number of times each one of the 32 drugs were in these intersections. Using the DRKG, we compare the drug repurposing results in Covid-19 among PanRep-FT that is finetuned in link prediction and the baseline RGCN. We employ $L = 1$ hidden layer with $D = 600$ and train for 800 epochs both networks. For each gene node we calculate with RGCN and PanRep-FT an inhibit link score associated with every drug. Based on this score, we rank all 'drug-inhibits-gene' triples per target gene. We obtain in this way 442 ranked lists of drugs, one per gene node. Finally, to assess whether our prediction is in par with the drugs used for treatment, we check the overlap among the top 100 predicted drugs and the drugs used in clinical trials per gene.

Table V lists the clinical drugs included in the top-100 predicted drugs across all the genes with their corresponding number of hits for the RGCN and PanRep-FT. Several of the widely used drugs in clinical trials appear high on the predicted list in both prediction. Furthermore, PanRep-FT reports a higher hit rate than RGCN, which corroborates the benefit of using the universal pretraining decoders. The universal representation endows PanRep with increased generalization power that allows for accurate link prediction performance when training data are extremely scarce as is the case of Covid-19. While this study, does not recommend specific drugs, it demonstrates a powerful deep learning methodology to prioritize existing drugs for further investigation, which holds the potential of accelerating therapeutic development for Covid-19.

C. Ablation study

Table IV reports an ablation study by using different decoder subsets. The OAG graph does not have a rich motif structure and thus we did not use the motif supervision there and it is excluded from the ablation study. PanRep that uses all decoders obtains the best performance. The HIM and MRW decoders and their combination exhibit the second best performance.

Next, we compare the cluster and recover supervision decoder to the attribute generation supervision that is employed by several GNN pretraining methods [53]. In this experiment we employ the setting of Sec. VI-A for node classification. The attribute generation supervision employs a 2-layer MLP network that attempts to reconstruct the original nodal attributes given the node embeddings. In Table VI we report the node classification accuracy for different number of clusters K considered in the CR supervision. The CR methods outperform the attribute generation method. One reason for this is that the GNN encoder already consideres the attributes in calculating the embeddings, and this supervision does not increase the predictive capacity of the model. On the other hand the clustering supervision allows the GNN to discover clusters of nodes with similar attributes and hence refines the learned embeddings.

VII. CONCLUSION

This paper develops a novel framework for unsupervised learning of universal node representations on heterogenous graphs termed. PanRep supervises the GNN encoder by decoders attuned to model the clustering of local node features, structural similarity among nodes, the local and intermediate neighborhood structure, and the mutual information among same-type nodes. To further facilitate cases where limited labels are available we implement PanRep-FT. Experiments in node classification and link prediction corroborate the competitive performance of the learned universal node representations compared to unsupervised and semi-supervised methods. Experiments on the DRKG showcase the advantage of the universal embeddings in drug repurposing.

REFERENCES

[1] T. N. Kipf and M. Welling, "Semi-supervised classification with graph convolutional networks," in *Proc. Int. Conf. on Learn. Represantions*, Toulon, France, Apr. 2017.
[2] Q. Wang, Z. Mao, B. Wang, and L. Guo, "Knowledge graph embedding: A survey of approaches and applications," *IEEE Transactions on Knowledge and Data Engineering*, vol. 29, no. 12, pp. 2724–2743, 2017.
[3] X. Wu, X. Zhu, G.-Q. Wu, and W. Ding, "Data mining with big data," *IEEE transactions on knowledge and data engineering*, vol. 26, no. 1, pp. 97–107, 2013.
[4] Y. Bengio, A. C. Courville, and P. Vincent, "Unsupervised feature learning and deep learning: A review and new perspectives," *CoRR, abs/1206.5538*, vol. 1, p. 2012, 2012.
[5] J. Devlin, M.-W. Chang, K. Lee, and K. Toutanova, "Bert: Pre-training of deep bidirectional transformers for language understanding," *arXiv preprint arXiv:1810.04805*, 2018.
[6] D. Erhan, Y. Bengio, A. Courville, P.-A. Manzagol, P. Vincent, and S. Bengio, "Why does unsupervised pre-training help deep learning?" *Journal of Machine Learning Research*, vol. 11, no. Feb, pp. 625–660, 2010.
[7] D. F. Gleich, "Pagerank beyond the web," *SIAM Review*, vol. 57, no. 3, pp. 321–363, 2015.

TABLE VI
ATTRIBUTE GENERATION SUPERVISION AGAINST CLUSTERING AND RECOVER SUPERVISION FOR DIFFERENT NUMBER OF CLUSTERS K.

Datasets	Metrics	Train %	ATTRIBUTE GENERATION	CR $K=2$	CR $K=4$	CR $K=5$	CR $K=10$
IMDB	Macro-F1	40%	17.52	29.52	31.94	**32.21**	31.22
		60%	17.53	30.75	34.50	**35.16**	34.19
		80%	17.30	3145	35.02	**35.66**	34.82
	Micro-F1	40%	35.66	38.51	39.40	**39.13**	38.38
		60%	35.70	38.83	41.02	**41.13**	40.03
		80%	35.07	39.54	41.16	**41.39**	40.66

[8] K. Kloster and D. F. Gleich, "Heat kernel based community detection," in *Proc. Intl. Conf. on Knowledge Disc. and Data Mining (KDD)*, 2014, pp. 1386–1395.

[9] R. A. Rossi and N. K. Ahmed, "Role discovery in networks," *IEEE Transactions on Knowledge and Data Engineering*, vol. 27, no. 4, pp. 1112–1131, 2014.

[10] C. Donnat, M. Zitnik, D. Hallac, and J. Leskovec, "Learning structural node embeddings via diffusion wavelets," in *Proc. Intl. Conf. on Knowledge Disc. and Data Mining (KDD)*, 2018.

[11] J. A. Suykens and J. Vandewalle, "Least squares support vector machine classifiers," *Neural processing letters*, vol. 9, no. 3, pp. 293–300, 1999.

[12] B. Yang, W.-t. Yih, X. He, J. Gao, and L. Deng, "Embedding entities and relations for learning and inference in knowledge bases," *arXiv preprint arXiv:1412.6575*, 2014.

[13] I. Goodfellow, Y. Bengio, A. Courville, and Y. Bengio, *Deep Learning*. MIT press Cambridge, 2016, vol. 1.

[14] F. Gama, E. Isufi, G. Leus, and A. Ribeiro, "Graphs, convolutions, and neural networks," *arXiv preprint arXiv:2003.03777*, 2020.

[15] M. M. Bronstein, J. Bruna, Y. LeCun, A. Szlam, and P. Vandergheynst, "Geometric deep learning: going beyond euclidean data," *IEEE Sig. Process. Mag.*, vol. 34, no. 4, pp. 18–42, 2017.

[16] M. Defferrard, X. Bresson, and P. Vandergheynst, "Convolutional neural networks on graphs with fast localized spectral filtering," in *Proc. Advances Neural Inf. Process. Syst.*, Barcelona, Spain, Dec. 2016, pp. 3844–3852.

[17] F. Gama, A. G. Marques, G. Leus, and A. Ribeiro, "Convolutional neural networks architectures for signals supported on graphs," *arXiv preprint arXiv:1805.00165*, 2018.

[18] V. N. Ioannidis, A. G. Marques, and G. B. Giannakis, "Tensor graph convolutional networks for multi-relational and robust learning," *IEEE Transactions on Signal Processing*, vol. 68, pp. 6535–6546, 2020.

[19] V. N. Ioannidis, A. G. Marques, and G. B. Giannakis, "A recursive multi-layer graph neural network architecture for processing network data," in *Proc. IEEE Int. Conf. Acoust., Speech, Sig. Process.*, London, England, May 2019.

[20] L. Ruiz, F. Gama, A. G. Marques, and A. Ribeiro, "Median activation functions for graph neural networks," *arXiv preprint arXiv:1810.12165*, 2018.

[21] V. N. Ioannidis, S. Chen, and G. B. Giannakis, "Efficient and stable graph scattering transforms via pruning," *IEEE Trans. Pattern Anal. Mach. Intel.*, 2020.

[22] W. L. Hamilton, R. Ying, and J. Leskovec, "Representation learning on graphs: Methods and applications," *arXiv preprint arXiv:1709.05584*, 2017.

[23] J. Tang, M. Qu, M. Wang, M. Zhang, J. Yan, and Q. Mei, "Line: Large-scale information network embedding," in *Proceedings of the 24th international conference on world wide web*, 2015, pp. 1067–1077.

[24] A. Ahmed, N. Shervashidze, S. Narayanamurthy, V. Josifovski, and A. J. Smola, "Distributed large-scale natural graph factorization," in *Proceedings of the 22nd international conference on World Wide Web*, 2013, pp. 37–48.

[25] S. Cao, W. Lu, and Q. Xu, "Grarep: Learning graph representations with global structural information," in *Proceedings of the 24th ACM international on conference on information and knowledge management*, 2015, pp. 891–900.

[26] M. Ou, P. Cui, J. Pei, Z. Zhang, and W. Zhu, "Asymmetric transitivity preserving graph embedding," in *Proceedings of the 22nd ACM SIGKDD international conference on Knowledge discovery and data mining*, 2016, pp. 1105–1114.

[27] A. Grover and J. Leskovec, "node2vec: Scalable feature learning for networks," in *Proceedings of the 22nd ACM SIGKDD international conference on Knowledge discovery and data mining*, 2016, pp. 855–864.

[28] B. Perozzi, R. Al-Rfou, and S. Skiena, "Deepwalk: Online learning of social representations," in *Proceedings of the 20th ACM SIGKDD international conference on Knowledge discovery and data mining*, 2014, pp. 701–710.

[29] A. J. Smola and R. I. Kondor, "Kernels and regularization on graphs," in *Learning Theory and Kernel Machines*. Springer, 2003, pp. 144–158.

[30] Z. Wu, S. Pan, F. Chen, G. Long, C. Zhang, and S. Y. Philip, "A comprehensive survey on graph neural networks," *IEEE Transactions on Neural Networks and Learning Systems*, 2020.

[31] P. Veličković, W. Fedus, W. L. Hamilton, P. Liò, Y. Bengio, and R. D. Hjelm, "Deep graph infomax," *arXiv preprint arXiv:1809.10341*, 2018.

[32] Y. Dong, N. V. Chawla, and A. Swami, "metapath2vec: Scalable representation learning for heterogeneous networks," in *Proceedings of the 23rd ACM SIGKDD international conference on knowledge discovery and data mining*, 2017, pp. 135–144.

[33] C. Shi, B. Hu, W. X. Zhao, and S. Y. Philip, "Heterogeneous information network embedding for recommendation," *IEEE Transactions on Knowledge and Data Engineering*, vol. 31, no. 2, pp. 357–370, 2018.

[34] J. Shang, M. Qu, J. Liu, L. M. Kaplan, J. Han, and J. Peng, "Meta-path guided embedding for similarity search in large-scale heterogeneous information networks," *arXiv preprint arXiv:1610.09769*, 2016.

[35] M. Belkin, I. Matveeva, and P. Niyogi, "Regularization and semi-supervised learning on large graphs," in *Proc. Annual Conf. Learning Theory*, vol. 3120. Banff, Canada: Springer, Jul. 2004, pp. 624–638.

[36] M. Belkin, P. Niyogi, and V. Sindhwani, "Manifold regularization: A geometric framework for learning from labeled and unlabeled examples," *J. Mach. Learn. Res.*, vol. 7, pp. 2399–2434, 2006.

[37] V. N. Ioannidis, M. Ma, A. Nikolakopoulos, G. B. Giannakis, and D. Romero, "Kernel-based inference of functions on graphs," in *Adaptive Learning Methods for Nonlinear System Modeling*, D. Comminiello and J. Principe, Eds. Elsevier, 2018.

[38] X. Zhu, Z. Ghahramani, and J. D. Lafferty, "Semi-supervised learning using gaussian fields and harmonic functions," in *Proc. Int. Conf. Mach. Learn.*, Washington, USA, Jun. 2003, pp. 912–919.

[39] D. I. Shuman, S. K. Narang, P. Frossard, A. Ortega, and P. Vandergheynst, "The emerging field of signal processing on graphs: Extending high-dimensional data analysis to networks and other irregular domains," *IEEE Sig. Process. Mag.*, vol. 30, no. 3, pp. 83–98, May 2013.

[40] E. Ceci, Y. Shen, G. B. Giannakis, and S. Barbarossa, "Graph-based learning under perturbations via total least-squares," *IEEE Transactions on Signal Processing*, vol. 68, pp. 2870–2882, 2020.

[41] E. Ceci and S. Barbarossa, "Graph signal processing in the presence of topology uncertainties," *IEEE Transactions on Signal Processing*, vol. 68, pp. 1558–1573, 2020.

[42] S. Segarra, A. G. Marques, G. Leus, and A. Ribeiro, "Reconstruction of graph signals through percolation from seeding nodes," *arXiv preprint arXiv:1507.08364*, 2015.

[43] V. N. Ioannidis, A. S. Zamzam, G. B. Giannakis, and N. D. Sidiropoulos, "Coupled graphs and tensor factorization for imputation and community detection," *IEEE Trans. on Knowledge and Data Engineering (Submitted Sep.)*, 2018.

[44] P. Veličković, G. Cucurull, A. Casanova, A. Romero, P. Lio, and Y. Bengio, "Graph attention networks," in *Proc. Int. Conf. on Learn. Represantions*, 2018.

[45] M. Schlichtkrull, T. N. Kipf, P. Bloem, R. Van Den Berg, I. Titov, and M. Welling, "Modeling relational data with graph convolutional networks," in *European Semantic Web Conference*. Springer, 2018, pp. 593–607.

[46] X. Fu, J. Zhang, Z. Meng, and I. King, "Magnn: Metapath aggregated graph neural network for heterogeneous graph embedding," in *Proceedings of The Web Conference 2020*, 2020, pp. 2331–2341.

[47] X. Wang, H. Ji, C. Shi, B. Wang, Y. Ye, P. Cui, and P. S. Yu, "Heterogeneous graph attention network," in *The World Wide Web Conference*, 2019, pp. 2022–2032.

[48] Y. Zhou, Y. Hou, J. Shen, Y. Huang, W. Martin, and F. Cheng, "Network-based drug repurposing for novel coronavirus 2019-ncov/sars-cov-2," *Cell discovery*, vol. 6, no. 1, pp. 1–18, 2020.

[49] V. N. Ioannidis, X. Song, S. Manchanda, M. Li, X. Pan, D. Zheng, X. Ning, X. Zeng, and G. Karypis, "Drkg - drug repurposing knowledge graph for covid-19," https://github.com/gnn4dr/DRKG/, 2020.

[50] D. Zheng, X. Song, C. Ma, Z. Tan, Z. Ye, J. Dong, H. Xiong, Z. Zhang, and G. Karypis, "Dgl-ke: Training knowledge graph embeddings at scale," *arXiv preprint arXiv:2004.08532*, 2020.

[51] J. Donahue, Y. Jia, O. Vinyals, J. Hoffman, N. Zhang, E. Tzeng, and T. Darrell, "Decaf: A deep convolutional activation feature for generic visual recognition," in *International conference on machine learning*, 2014, pp. 647–655.

[52] R. Girshick, J. Donahue, T. Darrell, and J. Malik, "Rich feature hierarchies for accurate object detection and semantic segmentation," in *Proceedings of the IEEE conference on computer vision and pattern recognition*, 2014, pp. 580–587.

[53] Z. Hu, Y. Dong, K. Wang, K.-W. Chang, and Y. Sun, "Gpt-gnn: Generative pre-training of graph neural networks," in *arxiv*, 2020.

[54] J. Qiu, Q. Chen, Y. Dong, J. Zhang, H. Yang, M. Ding, K. Wang, and J. Tang, "Gcc: Graph contrastive coding for graph neural network pre-training," in *arxiv*, 2020.

[55] W. Hu, B. Liu, J. Gomes, M. Zitnik, P. Liang, V. Pande, and J. Leskovec, "Strategies for pre-training graph neural networks," in *International Conference on Learning Representations*, 2019.

[56] J. Gilmer, S. S. Schoenholz, P. F. Riley, O. Vinyals, and G. E. Dahl, "Neural message passing for quantum chemistry," in *International Conference on Machine Learning*, 2017.

[57] P. W. Battaglia, J. B. Hamrick, V. Bapst, A. Sanchez-Gonzalez, V. Zambaldi, M. Malinowski, A. Tacchetti, D. Raposo, A. Santoro, R. Faulkner *et al.*, "Relational inductive biases, deep learning, and graph networks," *arXiv preprint arXiv:1806.01261*, 2018.

[58] M. Wang, L. Yu, D. Zheng, Q. Gan, Y. Gai, Z. Ye, M. Li, J. Zhou, Q. Huang, C. Ma *et al.*, "Deep graph library: Towards efficient and scalable deep learning on graphs," *arXiv preprint arXiv:1909.01315*, 2019.

[59] G. Yuan, P. K. Murukannaiah, Z. Zhang, and M. P. Singh, "Exploiting sentiment homophily for link prediction," in *Proceedings of the 8th ACM Conference on Recommender systems*, 2014, pp. 17–24.

[60] Y. Koren, R. Bell, and C. Volinsky, "Matrix factorization techniques for recommender systems," *Computer*, vol. 42, no. 8, pp. 30–37, 2009.

[61] N. K. Ahmed, J. Neville, R. A. Rossi, N. G. Duffield, and T. L. Willke, "Graphlet decomposition: Framework, algorithms, and applications," *Knowledge and Information Systems*, vol. 50, no. 3, pp. 689–722, 2017.

[62] T. Kanungo, D. M. Mount, N. S. Netanyahu, C. D. Piatko, R. Silverman, and A. Y. Wu, "An efficient k-means clustering algorithm: Analysis and implementation," *IEEE transactions on pattern analysis and machine intelligence*, vol. 24, no. 7, pp. 881–892, 2002.

[63] M. M. Babu, N. M. Luscombe, L. Aravind, M. Gerstein, and S. A. Teichmann, "Structure and evolution of transcriptional regulatory networks," *Current opinion in structural biology*, vol. 14, no. 3, pp. 283–291, 2004.

[64] R. D. Hjelm, A. Fedorov, S. Lavoie-Marchildon, K. Grewal, P. Bachman, A. Trischler, and Y. Bengio, "Learning deep representations by mutual information estimation and maximization," *arXiv preprint arXiv:1808.06670*, 2018.

[65] D. E. Rumelhart, G. E. Hinton, and R. J. Williams, "Learning representations by back-propagating errors," *Nature*, vol. 323, no. 6088, p. 533, 1986.

[66] Z. Zhang, P. Luo, C. C. Loy, and X. Tang, "Facial landmark detection by deep multi-task learning," in *European conference on computer vision*. Springer, 2014, pp. 94–108.

[67] Z. Chen, V. Badrinarayanan, C.-Y. Lee, and A. Rabinovich, "Gradnorm: Gradient normalization for adaptive loss balancing in deep multitask networks," *arXiv preprint arXiv:1711.02257*, 2017.

[68] K. Xu, W. Hu, J. Leskovec, and S. Jegelka, "How powerful are graph neural networks?" in *Proc. Int. Conf. on Learn. Represantions*, 2019.

[69] D. P. Kingma and J. L. Ba, "Adam: A method for stochastic optimization," in *Proc. Int. Conf. on Learn. Represantions*, San Diego, CA, USA, May 2015.

[70] www.imdb.com, 2020.

[71] www.openacademic.ai/oag/, 2020.

[72] D. M. Powers, "Evaluation: from precision, recall and f-measure to roc, informedness, markedness and correlation," *Journal of Machine Learning Technologies*, vol. 2, p. 37–63, 2011.

[73] A. Bordes, N. Usunier, A. Garcia-Duran, J. Weston, and O. Yakhnenko, "Translating embeddings for modeling multi-relational data," in *Neural Information Processing Systems (NIPS)*, 2013, pp. 1–9.

[74] D. Poole, "Simple embedding for link prediction in knowledge graphs," in *NeurIPS*, 2018.

[75] W. DS, F. YD, G. AC, L. EJ, M. A, G. JR, S. T, J. D, L. C, S. Z, A. N, I. I, L. Y, M. A, G. N, W. A, C. L, C. R, L. D, P. A, K. C, and W. M, "Drugbank 5.0: a major update to the drugbank database for 2018 nucleic acids res," *PubMed*, 2017.

[76] S. D, G. AL, L. D, J. A, W. S, H.-C. J, S. M, D. NT, M. JH, B. P, J. LJ, and von Mering C., "String v11: protein-protein association networks with increased coverage, supporting functional discovery in genome-wide experimental datasets." *PubMed*, 2019.

[77] S. Orchard, M. Ammari, B. Aranda, L. Breuza, L. Briganti, F. Broackes-Carter, N. H. Campbell, G. Chavali, C. Chen, N. Del-Toro *et al.*, "The mintact project—intact as a common curation platform for 11 molecular interaction databases," *Nucleic acids research*, vol. 42, no. D1, pp. D358–D363, 2014.

[78] K. C. Cotto, A. H. Wagner, Y.-Y. Feng, S. Kiwala, A. C. Coffman, G. Spies, A. Wollam, N. C. Spies, O. L. Griffith, and M. Griffith, "DGIdb 3.0: a redesign and expansion of the drug–gene interaction database," *Nucleic Acids Research*, vol. 46, no. D1, pp. D1068–D1073, 11 2017. [Online]. Available: https://doi.org/10.1093/nar/gkx1143

[79] D. E. Gordon, G. M. Jang, M. Bouhaddou, J. Xu, K. Obernier, M. J. O'meara, J. Z. Guo, D. L. Swaney, T. A. Tummino, R. Huttenhain *et al.*, "A sars-cov-2-human protein-protein interaction map reveals drug targets and potential drug-repurposing," *Nature*, 2020.